

Scientific Article

Quantification of Dosimetry Improvement With or Without Patient Surface Guidance



Ke Sheng, PhD, FAAPM, DABR,^{a,*} Minsong Cao, PhD,^b Andrew Godley, PhD,^c Mu-Han Lin, PhD,^c Lukas Henze, MEng,^d Laura Hammond, MSc,^e Laurence Delombaerde, PhD,^f Kirsten Hierholz, Dipl -Ing,^g and Jana Kouptsidis, MSc^g

^aDepartment of Radiation Oncology, University of California, San Francisco, California; ^bDepartment of Radiation Oncology, University of California, Los Angeles, California; ^cDepartment of Radiation Oncology, The University of Texas Southwestern Medical Center, Dallas, Texas; ^dCancer Center Berlin-Neukölln, Vivantes Klinikum Neukölln, Berlin, Germany; ^eRadiotherapy Department, Raigmore Hospital, Inverness, United Kingdom; ^fDepartment of Oncology, UZ Leuven, Leuven, Belgium; and ^gKlinikum Darmstadt GmbH, Institut für Radionkologie und Strahlentherapie, Darmstadt, Germany

Received 4 December 2023; accepted 21 June 2024

Purpose: Noncoplanar beams and arcs are routinely used to improve dosimetry for intracranial cases, but their application for extracranial cases has been hampered by the risk of collision. This has led to conservative beam selection whose impact on plan dosimetry has not been previously studied.

Methods and Materials: A full-body 3-dimensional patient surface was acquired using optical cameras for a single lung patient at the time of computed tomography simulation. Eight stereotactic body radiation therapy (SBRT) plans were created for the patient, with varying degrees of noncoplanarity and deliverability. The plans included volumetric modulated arc therapy and intensity modulated radiation therapy (IMRT) plans ranging from simple, coplanar arcs to multiple noncoplanar arcs and IMRT beams. A total of 70 fields were created across the 8 plans, of which 21 fields were undeliverable with a 5-cm buffer. Organs-at-risk (OARs) metrics including R50, Dmax 2 cm from the PTV, lung V20, and chest wall V30 were evaluated. Five expert SBRT dosimetrists from 5 institutions evaluated field deliverability, with or without the guidance of the clearance map.

Results: In the dosimetry evaluation, a clear trend in increasing dosimetric compactness and OAR sparing is observed with increasing plan noncoplanarity. R50, Dmax 2 cm, lung V20, and chest wall V30 decreased 41%, 39%, 43%, and 57%, respectively, from plan 1 (2 coplanar partial arcs) to plan 8 (19 noncoplanar IMRT beams). In the observer tests, the expert dosimetrists' ability to accurately discern beam deliverability because of collision significantly increases with the clearance map. The errors in predicting colliding fields were eliminated using the whole-body surface and clearance map, and the user was able to select fields based on plan quality and patient comfort instead of being overly conservative.

Conclusion: The study shows that incorporating a personalized, whole-body clearance map in the treatment planning workflow can facilitate the adoption of noncoplanar beams or arcs that benefit the SBRT plan dosimetry.

© 2024 The Author(s). Published by Elsevier Inc. on behalf of American Society for Radiation Oncology. This is an open access article under the CC BY-NC-ND license (<http://creativecommons.org/licenses/by-nc-nd/4.0/>).

Sources of support: The study was supported in part by a research grant from VisionRT.

*Corresponding author: Ke Sheng, PhD, FAAPM, DABR; Email: ke.sheng@ucsf.edu

<https://doi.org/10.1016/j.adro.2024.101570>

2452-1094/© 2024 The Author(s). Published by Elsevier Inc. on behalf of American Society for Radiation Oncology. This is an open access article under the CC BY-NC-ND license (<http://creativecommons.org/licenses/by-nc-nd/4.0/>).

Introduction

C-arm gantry systems are the most common type of external beam radiation therapy delivery device today. In contrast to ring gantry systems, where moving components are enclosed and the couch cannot rotate, they typically include a gantry with 1 degree of rotational freedom and a couch with a minimum of 3 translational and 1 rotational degrees of freedom. C-arm gantry systems are versatile in delivering a wide range of treatments with varying field sizes, body sites, and noncoplanarity.

With 1 degree of gantry rotation freedom, C-arm gantry systems can deliver coplanar radiation therapy with the patient couch stationary at zero degrees. However, what makes a C-arm gantry system versatile is its flexibility to deliver noncoplanar radiation therapy with a combination of gantry and couch rotations. Noncoplanar beams are essential in intracranial stereotactic radiosurgery (SRS) to significantly improve the dose gradient and reduce normal tissue doses.¹ Noncoplanar radiation therapy for body sites has been recently intensified for superior dosimetry using static intensity modulated radiation therapy (IMRT)²⁻¹⁴ and volumetric modulated arc therapy (VMAT)^{4,15,16} beams. These recent noncoplanar methods primarily solved the mathematical problems of selecting noncoplanar beams and arcs for optimal dosimetry. A common challenge still exists in defining the safe beam space that is free of collision.

Because of the exposed moving gantry, collision has been a nonnegligible concern in external beam radiation therapy using C-arm systems. Several methods have been conventionally employed to minimize the risk. These methods include pressure and proximity sensors, laser guard, and computer-aided design (CAD) modeling. These safety interlocks are triggered when the moving gantry is within a certain distance of the patient or couch, and the gantry motion is stopped to protect the patient and equipment. Because of their reactive nature, they do not prospectively prevent plans with potential collision beams from being generated, or present planners with the full range of options for plan improvement. Other solutions such as ClearCheck (RadFormation) assess the computed tomography (CT) and couch configuration for potential collisions during the planning process but do not assess all elements that may cause a collision (eg, the patient surface outside the volume of the CT scan).

For coplanar beams, the risk of collision is low and can usually be predicted for patients with extremely lateral tumors or large circumferences. The low frequency of collision is, therefore, manageable as long as conservative limits are placed on beam location and arc length. However, for noncoplanar radiation therapy, because of the couch rotation, the chance for the gantry to collide with the patient significantly increases, and with it, the potential for patient harm, equipment damage, treatment delay, and need for replanning. Moreover, prediction of the

collision can be unreliable because of the unintuitive visualization of the collision space for the C-arm systems. As a result, many dosimetrists avoid or minimize the use of noncoplanar beams outside intracranial SRS, despite their potential dosimetric benefit.

To address this challenge, collision prediction has been studied. To predict the collision, the geometry of the linac components and patients needs to be estimated. In the first computerized collision prediction study, Humm¹⁷ approximated the machine and patient geometry with simple geometric shapes, including cylinders and cuboids. The estimation was subsequently refined with more detailed geometric models.¹⁸⁻²¹ The geometry of the linac components can be assumed to be invariant without engineering modification to the system. However, substantial variation exists in the individual patient size, setup positions, setup devices, and the planning isocenter. Computerized collision prediction is inaccurate without such patient-specific information.

Nioutsikou et al²² extracted the patient surface information from planning CT for patient-specific collision prediction. However, planning CTs are typically limited to the region of interest for radiation therapy, where the collision is less likely to happen. Capturing the entire body length in CT would unnecessarily expose the patient to ionizing radiation and exceed the CT scan duration. Yu et al²³ studied the feasibility of using optical cameras to capture the patient surface for collision prediction. They found that the optically captured surfaces are well suited and accurate for collision modeling and prediction in treatment planning. However, the handheld 3-dimensional (3D) scanners used for human subject surface imaging were impractical for the clinical workflow. More recently, room-mounted 3D cameras have been investigated. These wide-angle cameras provide a large field of view sufficient for whole-body patient surface imaging in the simulation position. Therefore, they can be seamlessly integrated into the clinical workflow for collision modeling. A pertinent question to be answered is if the enhanced computerized collision prediction can be transferred into more use of noncoplanar beams for improved patient dosimetry. The case study is designed to answer that question.

Methods and Materials

A lung stereotactic body radiation therapy (SBRT) patient was selected for the study under UCLA IRB#12-001882. The patient received diagnosis of non-small cell lung cancer in the upper right lung. At the same session of acquiring the planning CT, 3D surface images were obtained with a pair of wide-angle 3D cameras (VisionRT) (Fig. 1). Like existing VisionRT cameras, structure IR lights were projected to the surface for

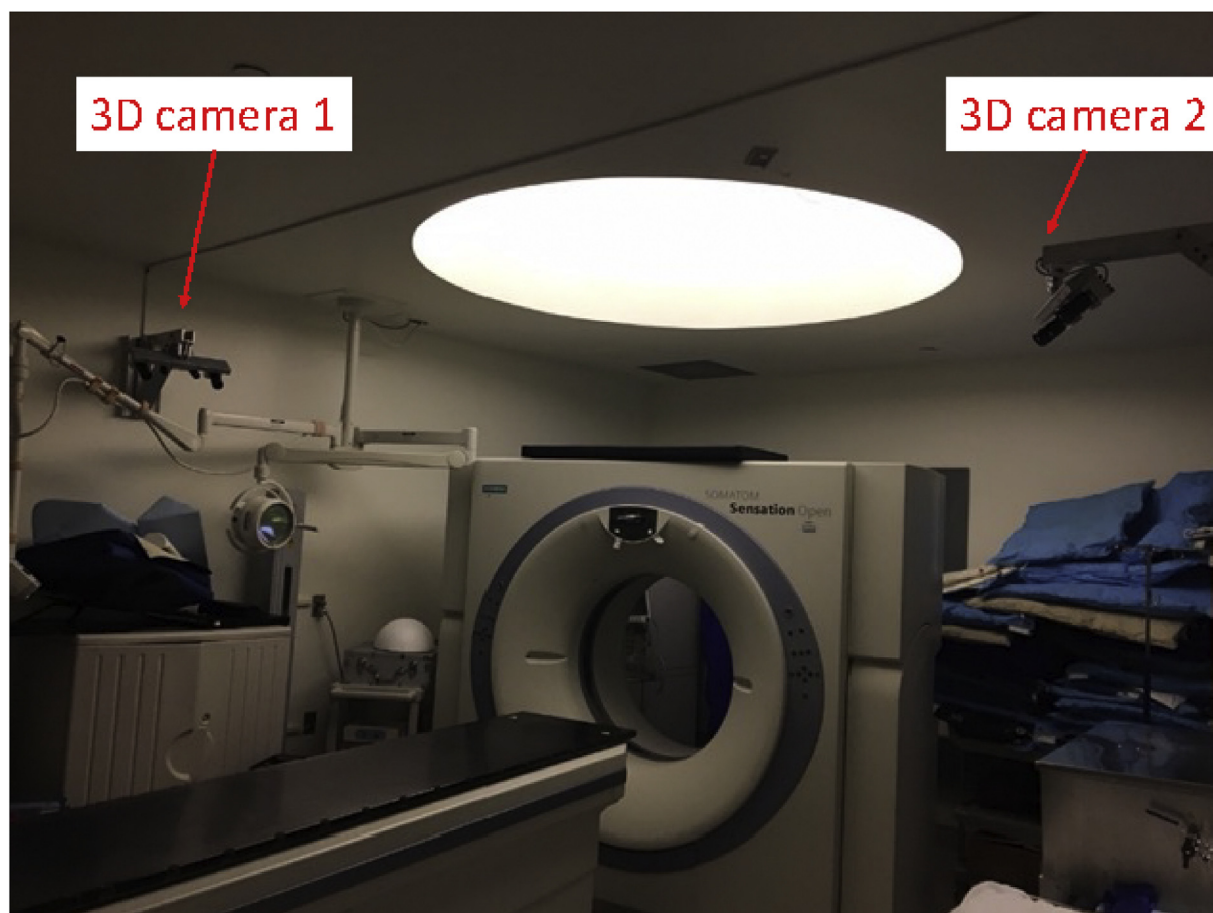


Figure 1 A pair of experimental wide-angle 3-dimensional cameras mounted on both sides of the computed tomography couch capture the entire patient length.

distance reconstruction. The field of view of the surface camera at the patient setup position is approximately 2 m. The accuracy of surface measurement has been determined to be under 2 mm using a cubic phantom. The 3D surface image acquisition took under 1 second.

Besides the optical surface measurement, a separate patient surface was also extracted from the CT and rigidly registered to the optical surface. The closest distances from the gantry and the patient surface with couch and gantry rotation are calculated based on the registered patient surface and the machine CAD model using MapRT (VisionRT). A margin or buffer in centimeter can be user-selected with a larger margin for a more conservative collision estimation. The simulation CT was transferred to the planning system (Eclipse, Varian) for treatment planning. Organs at risk (OARs), including the lung, heart, brachial plexus, bronchus, esophagus, and spinal cord, were contoured. The planning target volume (PTV) was generated by adding a 1-cm margin to the visible lung tumor. In total, 54 Gy/3 fractions were prescribed to cover 95% of the PTV using 6-MV X rays.

The patient was to be treated using a TrueBeam system (Varian Medical). The machine CAD model was obtained

via 3D scanning and postprocessing to model subcomponents and motion trajectories. The patient's optical surface was digitally processed to be separate from the CT couch. Registration of the optical and CT patient surfaces connected the optical surface with plan isocenter and subsequently the patient setup position. A clearance map was then created based on the patient and machine geometric model, as shown in Fig. 2.

The following 8 volumetric VMAT or IMRT plans were created for the patients as shown in Table 1: plans 1 to 6 were directly created in Eclipse; plans 7 to 8 were created first with automated 4π beam orientation optimization using the method published by O'Connor et al.²⁴ The beams as visualized in Fig. 3 were then imported into Eclipse for final optimization and dose calculation. In total, there are 70 individual arcs or fields for the 8 plans.

The trial was divided into 2 stages, with the first stage focusing on the dosimetry quality comparison among the 8 plans. We focused on the following metrics for the plan quality comparison without losing generality: R50 measuring the ratio between the 50% isodose volume and the PTV is considered one of the most important metrics for the quality of a lung SBRT plan. Smaller R50 indicates

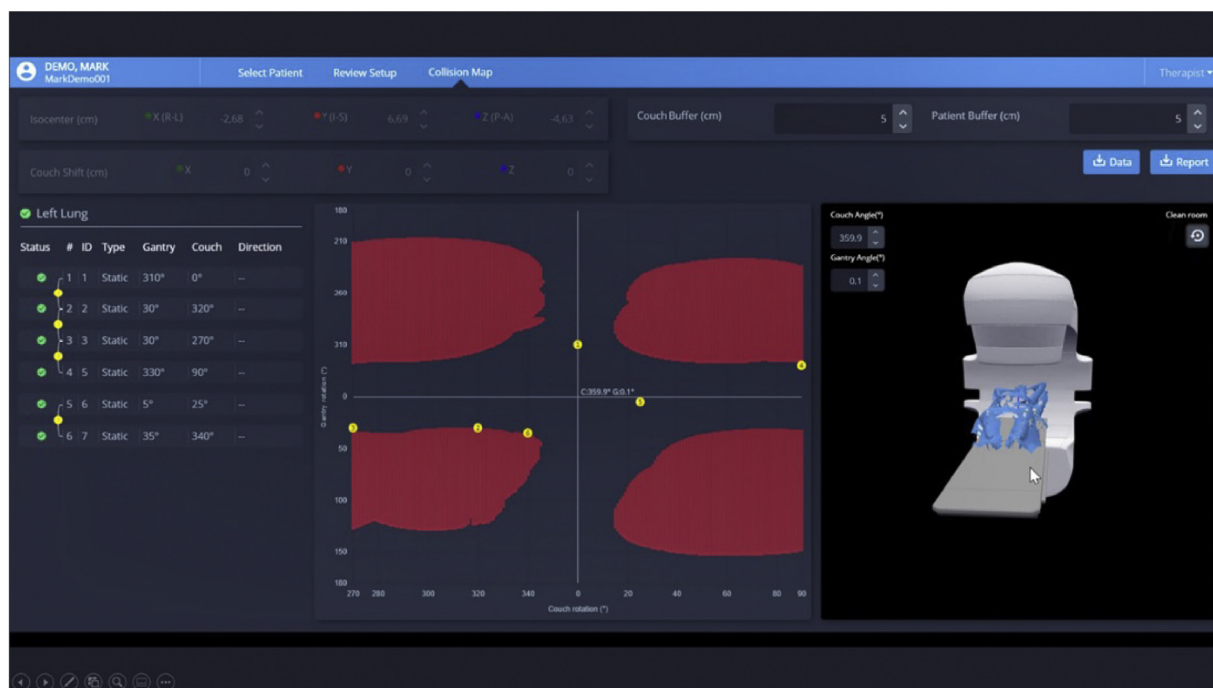


Figure 2 The patient surface image is registered with the machine model to calculate beam clearance, which is expressed as a 2D couch-gantry angle map using a pre-FDA version MapRT (VisionRT), which subsequently received FDA clearance in June 2023. Collision zones are shown in red. Yellow dots denote the individual beams. Beams causing collision with the user-defined buffer are highlighted in the left-side table. The right side shows the 3D rendering of the machine and patient surface. The couch and gantry can be maneuvered to achieve different positions corresponding to a specific beam for interactive viewing of the collision clearance.

Abbreviations: 2D = 2-dimensional; 3D = 3-dimensional; FDA = Food and Drug Administration.

more rapid dose falloff outside of the target and better sparing of the surrounding normal tissues from high-dose spillage.²⁵ Highly relevant to lung SBRT, the maximum dose 2 cm away from the PTV strongly correlates with treatment related to toxicities, particularly for patients with centrally located long tumors.²⁶ The third metric is lung V20, which has been correlated with the risk of

radiation-induced pneumonitis.²⁷ The last metric is chest wall V30, which has been correlated with the risk of severe chest wall pain and rib fracture.²⁸

In the second stage, 5 different reviewers from institutions across Europe and the United States with experience in planning noncoplanar lung SBRT plans were recruited to assess the individual field deliverability (with treatment

Table 1 Plan characteristics by coplanarity and collision

Plan ID	Technique	No. of coplanar beams/arcs	No. of noncoplanar beams/arcs	No. of beams/arcs colliding with a 5-cm buffer	No. of actual colliding beams/arcs
1	VMAT	2 partial	0	2	0
2	VMAT	2 full	0	2	0
3	VMAT	1	2	2	0
4	VMAT	1	2	3	1
5	IMRT	4	6	0	0
6	IMRT	4	6	0	1
7	IMRT	1	19	8	5
8	IMRT	1	19	4	0
Total		16	54	21	7

Abbreviations: IMRT = intensity modulated radiation therapy; VMAT = volumetric modulated arc therapy.

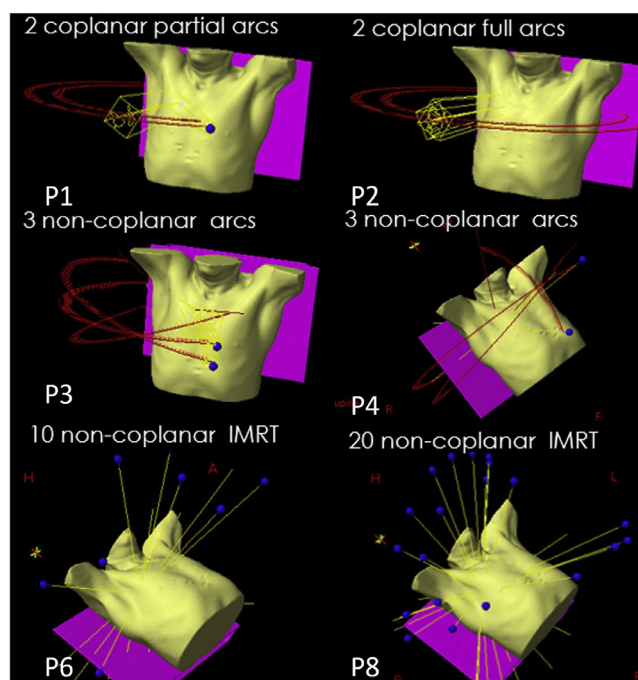


Figure 3 Beam arrangements for individual plans.

planning experience ranging from 3 to over 20 years). They were first requested to assess the deliverability without the clearance map and then with the clearance map. Using the clearance map, they were able to reduce the predefined 5-cm buffers for couch and patient individually based on their individual discretion and clinical experience. The number of correct and incorrect responses was documented.

Results

There is a clear trend of decreasing R50 with increasing plan noncoplanarity (Fig. 4). The trend is consistent with the observation from 4π lung SBRT optimization⁸ and with other metrics including maximum tissue dose 2 cm from the PTV, lung V20, and chest wall V30. The noncoplanar arc plans performed similarly to 10-field noncoplanar IMRT plans, whereas the 20 noncoplanar IMRT plans performed the best. Isodose comparisons between the least compact 2-partial arc VMAT and the most compact 4π plans are shown in Fig. 5. Both plans are deliverable without collision. The reduction of high-dose spillage with 4π radiation therapy is evident.

In the second stage, the ability for the experienced dosimetrists to determine collision situation with or without the clearance map was evaluated. Table 2 summarizes the results, where the users selected a buffer size based on their own clinical preferences (1 planner used 2-cm buffer, 3 planners used 3-cm buffer, and the final planner used 4-cm buffer). Without the clearance map, the dosimetrists were able to correctly identify most

nondeliverable beams (59 of 66, 89%), although the detection accuracy using the clearance map was 100%. There is a much larger difference for the deliverable beams. Without the clearance map, the dosimetrists tended to be more conservative and incorrectly rejected 101 beams (36% of all deliverable beams). In contrast, applying the clearance map, all nondeliverable plans were reliably identified by the collision map. Using additional data available from the clearance map, based on the visualization of the respective patient, and specifically the relationship between the gantry and the patient, the dosimetrists rejected 34 of the 284 deliverable beams (12%) because they felt that the gantry was too close to the patient, despite the fact that the map indicated no collision.

Discussion

The correlation between dose falloff outside the target and plan coplanarity has been well established for intracranial radiation, leading to the predominant use of noncoplanar beams in the brain SRS treatment.²⁹ There has been a similar motivation to improve the body radiation therapy conformality and compactness, particularly with the emergence of SBRT treatments. A dedicated SBRT system, CyberKnife,³⁰ was invented on a platform different than the conventional C-arm gantry. A lightweight linear accelerator was mounted on a robotic arm to deliver noncoplanar, nonisocentric treatments. Both systems showed distinct conformality improvements^{31,32} compared with coplanar treatment, but they were incompatible with IMRT and inefficient for treating larger

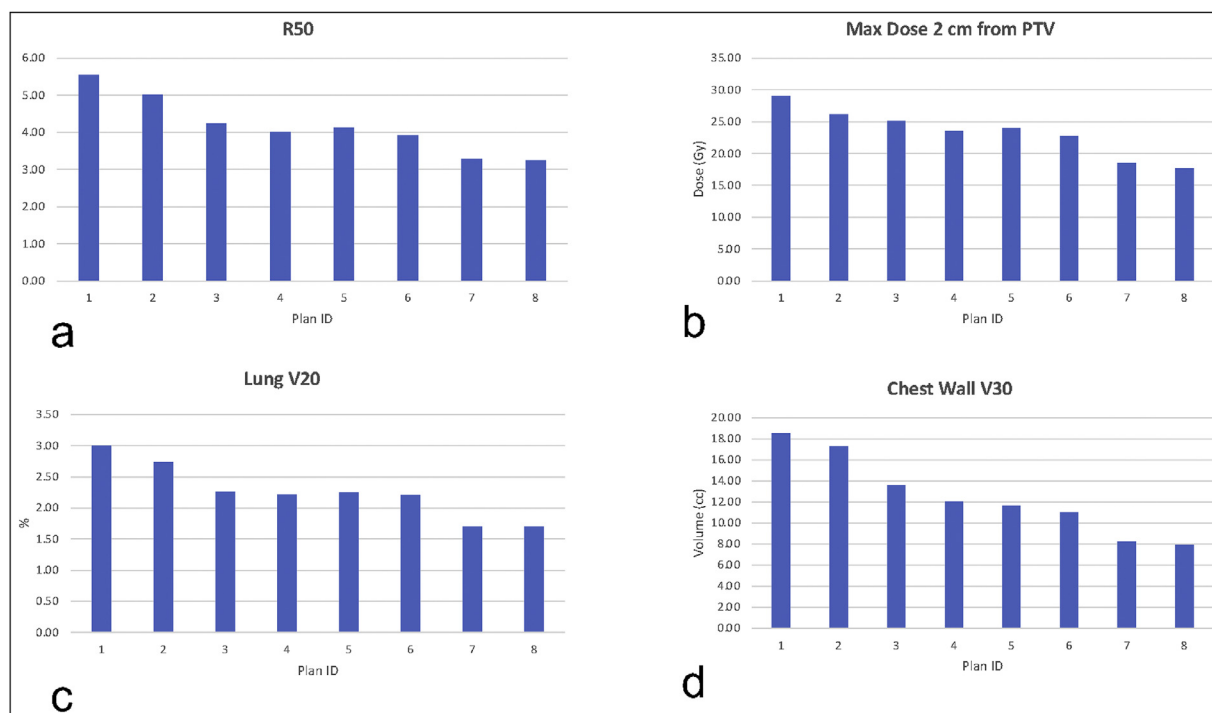


Figure 4 Organs-at-risk dosimetric comparison of the 8 plans.

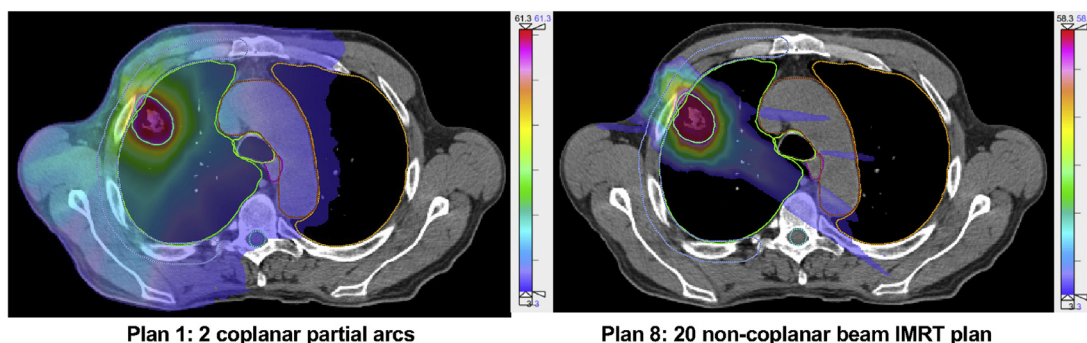


Figure 5 Isodose comparison of 2 deliverable plans.

tumors. However, noncoplanar geometry is less commonly used on the ubiquitous C-arm system for SBRT.

Chin et al³³ discussed the feasibility of improving treatment plan conformality using noncoplanar beams generated by a linac. With the availability of stereotactic localization and CT for 3D treatment planning, the idea was implemented for intracranial stereotactic radiosurgery (SRS).^{34,35} The advantages of noncoplanar geometry over coplanar geometry are evident in SRS cases. Feasibility studies of noncoplanar beams were extended to head and neck treatments and showed superior sparing of OARs, such as the parotid glands.^{36,37} Other than the greater demand for conformality in these cases, an important reason driving the earlier adoption in brain and head and neck tumors was the straightforward accessibility of

noncoplanar angles. In these cases, the entire hemisphere above the shoulders could be used for beam entrances without leading to a collision hazard. Other body sites are more challenging. Using a crude collision avoidance technique, Derycke et al³⁸ showed that for stage III lung cancer treatments, the spinal cord dose constraint could be satisfied if a simple noncoplanar beam arrangement was employed but not if coplanar beams were employed. Because of the significantly greater conformality from the noncoplanar beam arrangement, it became part of several Radiation Therapy Oncology Group (RTOG) SBRT protocols (RTOG 0236, 0618, and 0813).³⁹ Further studies have shown that noncoplanar beams generally improve dose conformality.^{40,41} The current study confirms the previous observation, and more extensive use of the

Table 2 Correctness of detecting the collision and subsequent beam deliverability with or without the clearance map

Ground truth—total no. of fields across all reviewers	Clinical assessment without clearance map		Clinical assessment with clearance map			
	Correct responses	Incorrect responses	Correct responses	Incorrect responses	With additional clinical discretion	
Ground truth Nondeliverable for chosen buffer size	66	59 (89%)	7 (11%)	66 (100%)	0(0%)	2/66 (3%)*
Ground truth Deliverable for chosen buffer size	284	183 (64%)	101 (36%)	284 (100%)	0 (0%)	34/284 (12%) [†]

*Respondent comment: the therapist will make small adjustments in the treatment room to make the gantry clear.
[†]Respondent comment: some fields were deliverable but considered too uncomfortable because of the machine near the patient's face.

noncoplanar beams significantly improves the dose compactness and reduces dose spillage and OAR doses. However, the enthusiasm for using noncoplanar geometry has not been translated into strong clinical adoption yet. First, human operators find it difficult to select high-quality noncoplanar beams using only experience and intuition.⁴² Second, noncoplanar beams may more likely lead to collisions and be undeliverable. Third, following current protocols, it takes significantly longer to deliver noncoplanar beams because of the additional patient maneuvering required by the therapists.

Solving the third challenge requires automation based on the solution of the first and second challenges. Currently, it is difficult for the dosimetrist to determine both the value and the clearance of a beam. This, in combination with additional therapists' effort and time for walking in the room when rotating the couch, is one reason for the slow clinical adoption. Templated noncoplanar arcs have been shown to be safe and efficient but are limited in disease sites.⁴³⁻⁴⁵

For more broadly applicable noncoplanar radiation therapy, the beam orientation optimization problem could be solved mathematically and computationally.^{2,5-9,15,46-48} It was also shown that a personalized clearance map can be achieved with a 3D camera-captured patient surface.²³ To our knowledge, the current study is the first to directly assess the human expert perception of the noncoplanar plans, with or without the assistance of a clearance map. Without the map as part of the planning interface, humans tend to be highly risk-averse, rejecting many collision-free beams (36% in the current study), which leads to reduced solution space and less-optimal treatment plans. The tediousness of assessing beam deliverability via dry run further discourages radiation oncology clinics from using these beams. On the contrary, with the explicit clearance map, the confidence, accuracy, and efficiency of beam selection all have improved, which could lead to the long anticipated broad acceptance of noncoplanar radiation therapy for body sites.

There are several limitations. First, the study is based on a single patient case and a small number of test plans. Although the results are consistent with previous

dosimetric studies and RTOG guidelines, a more extensive study including more plans and reviewers would strengthen the conclusion. Second, the reviewers were exposed to the clearance map in sequence and can develop bias because of the sequence. Nonetheless, the large effect size strongly supports the value of integrating a clearance map into the planning process. It is important to note that the accuracy and reliability of the clearance mapping solution has been studied outside this current study (data not shown).

Conclusions

The value of using patient-specific 3D surface for guiding lung SBRT planning using noncoplanar beams was assessed in the study. With the patient-specific collision map, the planners are better equipped to discern beams that are both safe to deliver and dosimetrically meritorious. The increased confidence led to acceptance of highly noncoplanar plans that significantly improved dose conformity and compactness that would have not been considered without the map.

Disclosures

Ke Sheng reports financial support was provided by VisionRT. Ke Sheng reports a relationship with VisionRT that includes: funding grants, speaking and lecture fees, and travel reimbursement. If there are other authors, they declare that they have no known competing financial interests or personal relationships that could have appeared to influence the work reported in this paper.

References

- Podgorsak EB, Pike GB, Olivier A, et al. Radiosurgery with high energy photon beams: a comparison among techniques. *Int J Radiat Oncol Biol Phys*. 1989;16:857-865.

2. Lyu Q, Neph R, Yu VY, et al. Many-isocenter optimization for robotic radiotherapy. *Phys Med Biol.* 2020;65: 045003.
3. Tran A, Zhang J, Woods K, et al. Treatment planning comparison of IMPT, VMAT and 4pi radiotherapy for prostate cases. *Radiat Oncol.* 2017;12:10.
4. Woods K, Nguyen D, Tran A, et al. Viability of non-coplanar VMAT for liver SBRT as compared to coplanar VMAT and beam orientation optimized 4pi IMRT. *Adv Radiat Oncol.* 2016;1:67-75.
5. Rwigema JC, Nguyen D, Heron DE, et al. 4pi noncoplanar stereotactic body radiation therapy for head-and-neck cancer: potential to improve tumor control and late toxicity. *Int J Radiat Oncol Biol Phys.* 2015;91:401-409.
6. Dong P, Nguyen D, Ruan D, et al. Feasibility of prostate robotic radiation therapy on conventional C-arm linacs. *Pract Radiat Oncol.* 2014;4:254-260.
7. Nguyen D, Dong P, Long T, et al. Integral dose investigation of non-coplanar treatment beam geometries in radiotherapy. *Med Phys.* 2014;41: 011905.
8. Dong P, Lee P, Ruan D, et al. 4pi noncoplanar stereotactic body radiation therapy for centrally located or larger lung tumors. *Int J Radiat Oncol Biol Phys.* 2013;86:407-413.
9. Dong P, Lee P, Ruan D, et al. 4pi non-coplanar liver SBRT: a novel delivery technique. *Int J Radiat Oncol Biol Phys.* 2013;85:1360-1366.
10. Rossi L, Breedveld S, Aluwini S, et al. Noncoplanar beam angle class solutions to replace time-consuming patient-specific beam angle optimization in robotic prostate stereotactic body radiation therapy. *Int J Radiat Oncol Biol Phys.* 2015;92:762-770.
11. Voet PW, Dirckx ML, Breedveld S, et al. Automated generation of IMRT treatment plans for prostate cancer patients with metal hip prostheses: comparison of different planning strategies. *Med Phys.* 2013;40: 071704.
12. Voet PW, Breedveld S, Dirckx ML, et al. Integrated multicriterial optimization of beam angles and intensity profiles for coplanar and noncoplanar head and neck IMRT and implications for VMAT. *Med Phys.* 2012;39:4858-4865.
13. Schipaanboord BWK, Heijmen BJM, Breedveld S. TBS-BAO: fully automated beam angle optimization for IMRT guided by a total-beam-space reference plan. *Phys Med Biol.* 2022:67.
14. Ventura T, Rocha H, da Costa Ferreira B, et al. Comparison of two beam angular optimization algorithms guided by automated multicriterial IMRT. *Phys Med.* 2019;64:210-221.
15. Lyu Q, Yu VY, Ruan D, et al. A novel optimization framework for VMAT with dynamic gantry couch rotation. *Phys Med Biol.* 2018;63: 125013.
16. Leitao J, Bijman R, Wahab Sharfo A, et al. Automated multi-criterial planning with beam angle optimization to establish non-coplanar VMAT class solutions for nasopharyngeal carcinoma. *Phys Med.* 2022;101:20-27.
17. Humm JL. Collision avoidance in computer optimized treatment planning. *Med Phys.* 21:1053-1064.
18. Humm JL, Pizzuto D, Fleischman E, et al. Collision detection and avoidance during treatment planning. *Int J Radiat Oncol Biol Phys.* 1995;33:1101-1108.
19. Tsiakalos MF, Scherebmann E, Theodorou K, et al. Graphical treatment simulation and automated collision detection for conformal and stereotactic radiotherapy treatment planning. *Med Phys.* 28:1359-1363.
20. Chao MM, Chao LS, Chen YJ, et al. Image display for collision avoidance of radiation therapy: treatment planning. *J Digit Imaging.* 2001;14:186-191.
21. Becker SJ. Collision indicator charts for gantry-couch position combinations for Varian linacs. *J Appl Clin Med Phys.* 2011;12:3405.
22. Nioutsikou E, Bedford JL, Webb S. Patient-specific planning for prevention of mechanical collisions during radiotherapy. *Phys Med Biol.* 2003;48:N313-N321.
23. Yu VY, Tran A, Nguyen D, et al. The development and verification of a highly accurate collision prediction model for automated non-coplanar plan delivery. *Med Phys.* 2015;42:6457-6467.
24. O'Connor D, Yu V, Nguyen D, et al. Fraction-variant beam orientation optimization for non-coplanar IMRT. *Phys Med Biol.* 2018;63: 045015.
25. Timmerman RD, Hu C, Michalski JM, et al. Long-term results of stereotactic body radiation therapy in medically inoperable stage I non-small cell lung cancer. *JAMA Oncol.* 2018;4:1287-1288.
26. Bezjak A, Paulus R, Gaspar LE, et al. Safety and efficacy of a five-fraction stereotactic body radiotherapy schedule for centrally located non-small-cell lung cancer: NRG oncology/RTOG 0813 trial. *J Clin Oncol.* 2019;37:1316-1325.
27. Tsujino K, Hirota S, Endo M, et al. Predictive value of dose-volume histogram parameters for predicting radiation pneumonitis after concurrent chemoradiation for lung cancer. *Int J Radiat Oncol Biol Phys.* 2003;55:110-115.
28. Dunlap NE, Cai J, Biedermann GB, et al. Chest wall volume receiving >30 Gy predicts risk of severe pain and/or rib fracture after lung stereotactic body radiotherapy. *Int J Radiat Oncol Biol Phys.* 2010;76:796-801.
29. Leksell L. The stereotaxic method and radiosurgery of the brain. *Acta Chir Scand.* 1951;102:316-319.
30. Adler Jr. JR, Chang SD, Murphy MJ, et al. The Cyberknife: a frameless robotic system for radiosurgery. *Stereotact Funct Neurosurg.* 1997;69:124-128.
31. Brown WT, Wu X, Amendola B, et al. Treatment of early non-small cell lung cancer, stage IA, by image-guided robotic stereotactic radioablation—CyberKnife. *Cancer J.* 2007;13:87-94.
32. Oermann EK, Suy S, Hanscom HN, et al. Low incidence of new biochemical and clinical hypogonadism following hypofractionated stereotactic body radiation therapy (SBRT) monotherapy for low- to intermediate-risk prostate cancer. *J Hematol Oncol.* 2011;4:12.
33. Chin LM, Siddon RL, Svensson GK, et al. Progress in 3-D treatment planning for photon beam therapy. *Int J Radiat Oncol Biol Phys.* 1985;11:2011-2020.
34. Schlegel W, Pasty O, Bortfeld T, et al. Computer systems and mechanical tools for stereotactically guided conformation therapy with linear accelerators. *Int J Radiat Oncol Biol Phys.* 1992;24:781-787.
35. Kooy HM, Nedzi LA, Loeffler JS, et al. Treatment planning for stereotactic radiosurgery of intra-cranial lesions. *Int J Radiat Oncol Biol Phys.* 1991;21:683-693.
36. Nutting CM, Rowbottom CG, Cosgrove VP, et al. Optimisation of radiotherapy for carcinoma of the parotid gland: a comparison of conventional, three-dimensional conformal, and intensity-modulated techniques. *Radiother Oncol.* 2001;60:163-172.
37. Marsh L, Eisbruch A, Watson B, et al. Treatment planning for parotid sparing in the patient requiring bilateral neck irradiation. *Med Dosim.* 1996;21:7-13.
38. Derycke S, Van Duyse B, De Gerssem W, et al. Non-coplanar beam intensity modulation allows large dose escalation in stage III lung cancer. *Radiother Oncol.* 1997;45:253-261.
39. Timmerman R, Kavanagh B. *Stereotactic body radiation therapy.* Lippincott Williams & Wilkins; 2004.
40. Lam S, Rogers L, Wichman B. Non-coplanar inverse planning IMRT using the MIMiC system: clinical significance in choice of 2-cm/1-cm mode and single couch vs. multiple couch angles. *Med Dosim.* 2001;26:11-15.
41. de Pooter JA, Mendez Romero A, Jansen WP, et al. Computer optimization of noncoplanar beam setups improves stereotactic treatment of liver tumors. *Int J Radiat Oncol Biol Phys.* 2006;66:913-922.
42. Ferreira BC, Svensson R, Lof J, et al. The clinical value of non-coplanar photon beams in biologically optimized intensity modulated dose delivery on deep-seated tumours. *Acta Oncol.* 2003;42:852-864.
43. Vergalasova I, Liu H, Alonso-Basanta M, et al. Multi-institutional dosimetric evaluation of modern day stereotactic radiosurgery (SRS)

- treatment options for multiple brain metastases. *Front Oncol.* 2019;9:483.
44. Woods KE, Ma TM, Cook KA, et al. A prospective phase II study of automated non-coplanar VMAT for recurrent head and neck cancer: initial report of feasibility, safety, and patient-reported outcomes. *Cancers (Basel).* 2022:14.
 45. Woods K, Chin RK, Cook KA, et al. Automated non-coplanar VMAT for dose escalation in recurrent head and neck cancer patients. *Cancers (Basel).* 2021:13.
 46. MacDonald RL, Syme A, Little B, et al. Toward the combined optimization of dynamic axes (CODA) for stereotactic radiotherapy and radiosurgery using fixed couch trajectories. *Med Phys.* 2020;47:307-316.
 47. Landers A, O'Connor D, Ruan D, et al. Automated 4pi radiotherapy treatment planning with evolving knowledge-base. *Med Phys.* 46:3833-3843.
 48. Nguyen D, Rwigema JC, Yu VY, et al. Feasibility of extreme dose escalation for glioblastoma multiforme using 4pi radiotherapy. *Radiat Oncol.* 2014;9:239.